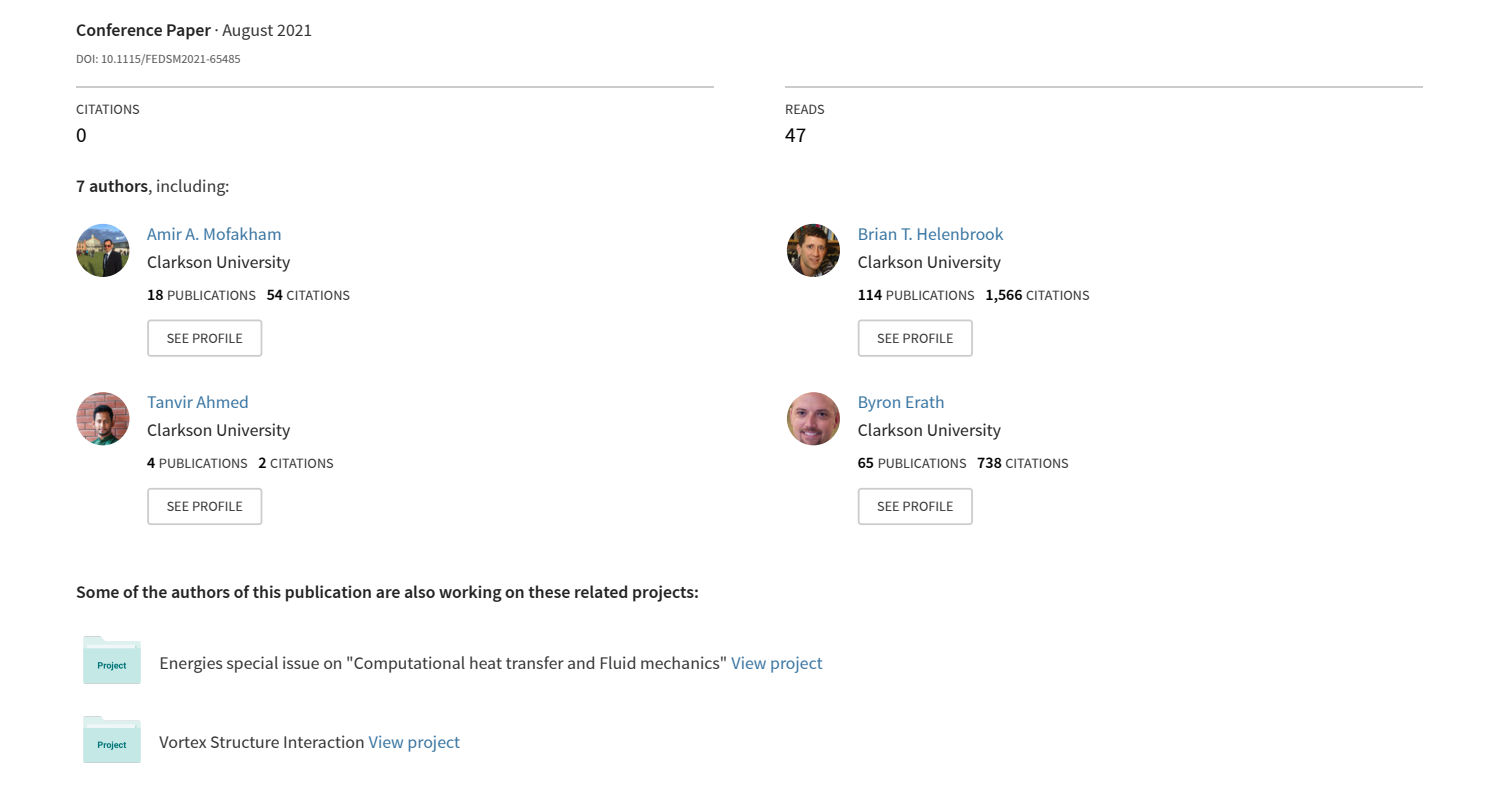
Significance of Vocal Tract Geometrical Variations and Loudness on Airflow and Droplet Dispersion in a Two-Dimensional Representation of [F]



FEDSM-65485

SIGNIFICANCE OF VOCAL TRACT GEOMETRICAL VARIATIONS AND LOUDNESS ON AIRFLOW AND DROPLET DISPERSION IN A TWO-DIMENSIONAL REPRESENTATION OF [F]

Amir A. Mofakham

Department of Mechanical and Aeronautical Engineering Clarkson University Potsdam, NY 13699 Email: abdolla@clarkson.edu

Tanvir Ahmed

Department of Mechanical and Aeronautical Engineering Clarkson University Potsdam, NY 13699 Email:tanvahm@clarkson.edu

Andrea R. Ferro

Department of Civil and Environmental Engineering Clarkson University Potsdam, NY 13699 Email: aferro@clarkson.edu

Brian T. Helenbrook

Department of Mechanical and Aeronautical Engineering Clarkson University Potsdam, NY 13699 Email: bhelenbr@clarkson.edu

Byron D. Erath

Department of Mechanical and Aeronautical Engineering Clarkson University Potsdam, NY 13699 Email: berath@clarkson.edu

Deborah M. Brown

Joint Educational Programs
Trudeau Institute
Saranac Lake, NY 12983
Email: dbrown@trudeauinstitute.org

Goodarz Ahmadi

Department of Mechanical and Aeronautical Engineering Clarkson University Potsdam, NY 13699 Email: gahmadi@clarkson.edu

ABSTRACT

The significance of respiratory droplet transmission in spreading respiratory diseases such as COVID-19 has been identified by researchers. Although one cough or sneeze generates a

large number of respiratory droplets, they are usually infrequent. In comparison, speaking and singing generate fewer droplets, but occur much more often, highlighting their potential as a vector for airborne transmission. However, the flow dynamics of

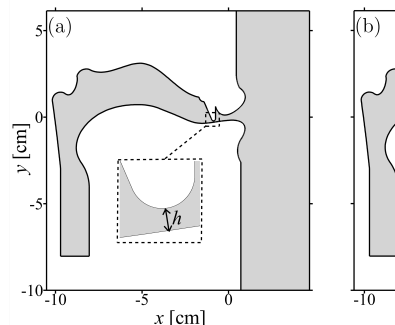
speech and the transmission of speech droplets have not been fully investigated. To shed light on this topic, two-dimensional geometries of a vocal tract for a labiodental fricative [f] were generated based on real-time MRI of a subject during pronouncing [f]. In these models, two different curvatures were considered for the tip tongue shape and the lower lip to highlight the effects of the articulator geometries on transmission dynamics. The commercial ANSYS-Fluent CFD software was used to solve the complex expiratory speech airflow trajectories. Simultaneously, the discrete phase model of the software was used to track submicron and large size respiratory droplets exhaled during [f] utterance. The simulations were performed for high, normal, and low lung pressures to explore the influence of loud, normal, and soft utterances, respectively, on the airflow dynamics. The presented results demonstrate the variability of the airflow and droplet propagation as a function of the vocal tract geometrical characteristics and loudness.

INTRODUCTION

The aerosol transmission was finally recognized as a mode of transmission of SARS-CoV-2, the virus that causes COVID-19, [1, 2]. Respiratory aerosols are produced as people breathe, talk, sing, cough, and/or sneeze. Recent investigations have identified the potential of speech flow in generating large fluid velocities [3] and the role of speech in producing expiratory droplets [4]. However, the variations of speech flow as a function of utterance type, loudness, and vocal tract geometry have not been fully understood. Therefore, in this investigation, the expirated flow for a fricative [f] (e.g., front) were explored. Fricatives are consonant sounds that are produced by passing expiratory flow through a constriction opening in the vocal tract. As a result of having the constriction, expiratory airflow trajectories with large velocities are produced during fricative pronunciations with a high potential to produce and transmit respiratory droplets. The influence of loudness on the rate of respiratory droplet generation was reported earlier [5] and preliminary investigations showed the remarkable effects of vocal tract geometrical variations on speech flow [6]. Accordingly, airflow trajectories and droplet propagation were investigated in this work as a function of loudness and vocal tract geometry. To clarify the propagation pattern of different sizes of droplets in expiratory flow, 0.1 to $50\ \mu m$ spherical droplets were introduced at the constriction region and their trajectories were evaluated during the flow simulations. The results were used to assess the risk of short and long-range aerosol transmission.

VOCAL TRACT MODELS

Two-dimensional generalized models of the vocal tract were produced based on real-time magnetic resonance imaging (MRI) data [7] of a male subject during articulation of the fricative con-



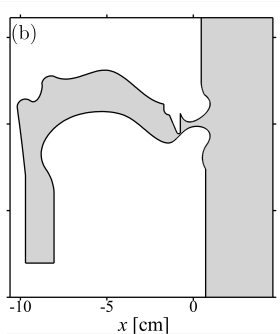


FIGURE 1. VOCAL TRACT GEOMETRIES OF (a) FLAT-[F] AND (b) CURVED-[F] MODELS.

sonant [f], as shown in Figure 1. Oral geometry is highly variable among different subjects, but the most critical parts of the vocal tract of [f] are the labiodental constriction, the position of teeth relative to the lower lip, and the lower lip. The labiodental constriction is generated by positioning the lower lip adjacent to the upper tooth during the pronunciation of [f] utterance. Assuming the width of the mouth is 2.5 cm, the minimum height of the labiodental constriction (h) which is shown in the inset of Figure 1.a was adjusted to 0.8 mm based on the average crosssectional area of 0.2 cm² reported from physiological investigations [8]. Variations in the geometry of the mouth during particular utterances occur based on the preceding and succeeding sounds that are produced, as well as the intonation or the stress of the speaker [6,9]. Intra-subject variability can also produce different vocal tract geometries for the same utterance. Even during the successive articulation of [f] in different incidents by the same subject, the location of the upper teeth relative to the lower lip varies. To highlight the influence of the vocal tract geometrical variations on the expirated flow, two different vocal tract models were generated based on two different tip tongue curvatures. Figure 1.a illustrates the flat-[f] model where the curvature of the tip tongue and the lower lip is flatter when compared to that of the curved-[f], where the tooth is positioned at a location where there is a steep upward slope, as shown in Figure 1.b.

NUMERICAL MODEL

In order to quantify the speech airflow expirated from the mouth cavity, the flow was simulated using the laminar unsteady model of the ANSYS-Fluent computational fluid dynamics (CFD) software by solving the two-dimensional Navier-Stokes and continuity governing equations in the computational domain shown in Figure 2. Constant pressure (i.e., constant loudness) was applied at the inlet of the domain, which is located below the glottis, as shown in Figure 2. To discretize the domain, it was divided into different sections where the grid size was set

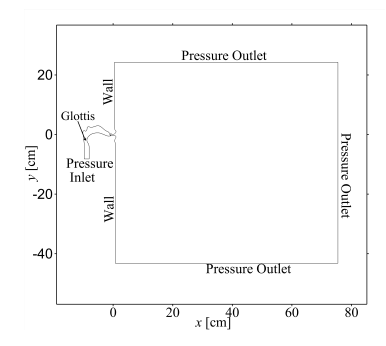


FIGURE 2. COMPUTAIONAL DOMAIN AND BOUNDARY CONDITIONS.

properly to assure that the computational grid was refined enough to yield accurate estimations of the complex speech flow structures. For instance, the maximum grid size in the constriction region was set to 1×10^{-5} , where a refined grid is needed to accurately resolve vortical structures at the mouth exit significantly impacting the behavior of the expiratory flow. The size of the cells was gradually increased to 1×10^{-3} in the far-field area. For more information regarding the mesh generation procedure, grid study, and accuracy justifications, interested readers are referred to [10]. The simulations were carried out with a quiescent initial condition and a time step of 1×10^{-5} s. To highlight the effects of the speaker loudness on the airflow and droplet propagation during speaking, the simulations were conducted with three different constant inlet pressures of 300, 600, and 860 Pa representing soft, normal, and loud speech, respectively.

To investigate the expiration of respiratory droplets during speech, simultaneously, the discrete phase model (DPM) of the ANSYS-Fluent software was used to solve the equation of motion of droplets including the gravity in the -y direction and the drag forces to track respiratory droplets produced at the tooth gap area with diameters of 0.1, 1, 5, 10, 20, and 50 μ m and a density of 1,030 kg/m³. A user-defined function (UDF) was implemented into the code to set the initial velocities of droplets equal to that of the local fluid. Trap and escape boundary conditions were imposed on the walls and the outlets, respectively. It was assumed that droplets are spherical with a constant diameter (no evaporation). The concentration of the droplets was assumed to be small so that there was no interaction of droplets with each other and the flow was not affected by droplets.

COMPLEXITY OF EXPIRATED FLOW

Figure 3.a, 3.b, and 3.c, show snapshots of the instantaneous velocity contours at $t=0.1,\,0.2,\,$ and 0.4 s, respectively, for the flat [f] model with an inlet pressure of 600 Pa, which is representative of normal speech loudness. Velocity vectors are superimposed on the velocity contours. The simulation re-

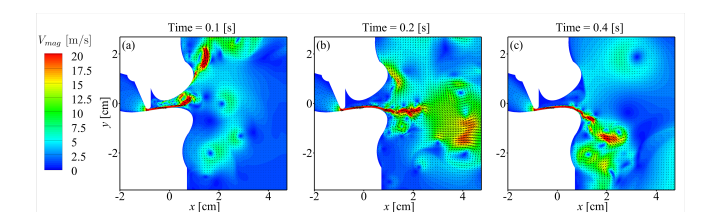


FIGURE 3. A SNAPSHOT OF THE INSTANTANEOUS VELOCITY CONTOURS AT (a) 0.1, (b) 0.2, AND (c) 0.4 s.

sults revealed that during the sustained pronunciation of [f], a jet flow with a maximum velocity of more than 30 m/s appears at the tooth gap exit propagating into the front field of the speaker through the gap area between the lips. The large velocity of the jet flow highlights the significant potential of speech in generating and spreading respiratory droplets. In addition, as seen in Figure 3, the jet flow is clearly unstable and unsteady with a trajectory that varies in time. The temporal evolution of the flow is such that the trajectory is mainly upward at 0.1 s, but it becomes almost horizontal at 0.2 s, and eventually downward at 0.4 s.

To better understand the evolution of the airflow trajectory, the angle of the jet in relative to the horizontal axis is evaluated in time and plotted versus time in Figure 4.a. As seen in the figure, the jet initially tends to attach to the upper lip propagating flow in the upward direction. However, at around 0.15 s, it migrates toward the lower lip assuming a horizontal orientation for a duration of about 0.5 s. Thereafter, it skews toward the lower lip and stays attached to the lower lip as evidenced by the negative airflow trajectories. The mean jet angle throughout the 0.4 s utterance is approximately zero degrees (-0.04°) , while the standard deviation is $\sim +30^{\circ}$. The large value of the standard variation is due to the temporal evolution of the flow, as well as the significant unsteadiness, which is observed by the small time-scale fluctuations observed in Figure 4.a. The instability of speech flow is due to the generation of vortices as a result of the jet interaction with the lips surfaces, and later the interruption of the jet flow exiting from the mouth by the vortex structures propagated earlier into the front-field area.

Since there is not a single modal for the expiration trajectories, the mean value does not represent the predominant airflow trajectories. Hence, the normalized histogram diagram of the expiration trajectories is also plotted in Figure 4.b as bar plots. The size of the bins is 5° and the heights of the bars represent the fraction of all the trajectories (N/N_t) fall into each range (bar). The figure confirms that the predominant direction of the jet in the initial duration of 0.4 s is downward with an angle around -20° . These findings suggest that a steady horizontal jet flow is not a good representation of the complex unsteady flow so that employing a steady horizontal model does not lead to an accurate estimation of speech flow.

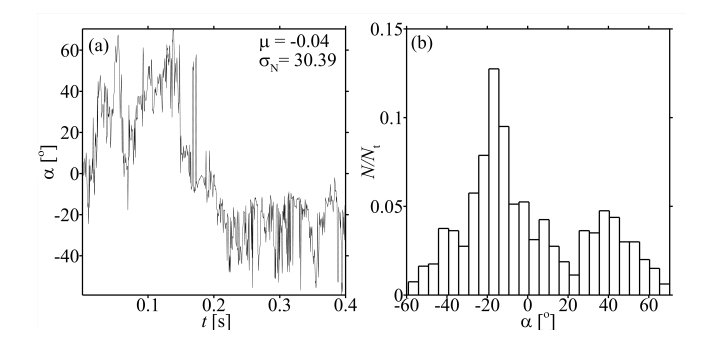


FIGURE 4. (a) THE JET ANGLE VARIATION DURING 0.4 s. (b) THE HISTOGRAM DISTRIBUTIONS OF THE JET ANGLE VARIATION.

EFFECT OF LOUDNESS

To investigate the influence of loudness on the expiration flow, the evolution and the histogram distribution of the jet flow trajectories for soft ($p_s = 300 \text{ Pa}$) and loud speech ($p_s = 860 \text{ Pa}$) are plotted in Figures 5.a-b and Figures 5.c-d, respectively. Comparing the jet angle evolution of soft and loud loudness depicted in Figure 5.a and 5.c, respectively, reveals that for soft loudness, the jet moves towards the lower lips in a short period of time (0.04 s), but the jet of loud loudness maintains airflow trajectories with positive angles for a longer period of time (0.1 s). The mean value of angle distribution of soft utterance is -9.14° with an angle of approximately -40° at t = 0.2 s, but the mean value of loud utterance is 14.75° with an angle of approximately -10° . The comparison of the histogram distribution of soft and loud loudness shown in Figures 5.b and 5.d clearly confirms that the reduction of loudness leads to having airflow trajectories with more negative angles, but the increase of the loudness increases the number of airflow trajectories with positive angles.

GEOMETRICAL VARIATION EFFECTS

To clarify the influence of the vocal tract geometrical variation, the mean velocity contours at 0.2 s in conjunction with the corresponding mean velocity vectors of the flat-[f] and the curved-[f] models (see Figure 1) are illustrated in Figure 6.a and 6.b, respectively. The mean velocities are the time average of the fluid velocities from 0.2 s simulation of the models starting from a quiescent state with a subglottal pressure of 600 Pa. The figures reveal the distinct differences in the airflow trajectories produced from the flat model and those of the curved model. Due to the variations of the jet angle at the mouth exit, which were previously mentioned in the discussion of Figure 3, a predominant direction is not detectable for airflow trajectories in Figure 6.a, but based on the snapshot of the instantaneous velocity contours at 0.2 s shown in Figure 3, it is known that the jet is mainly horizontal at 0.2 s. However, for the curved model, Figure 6.b

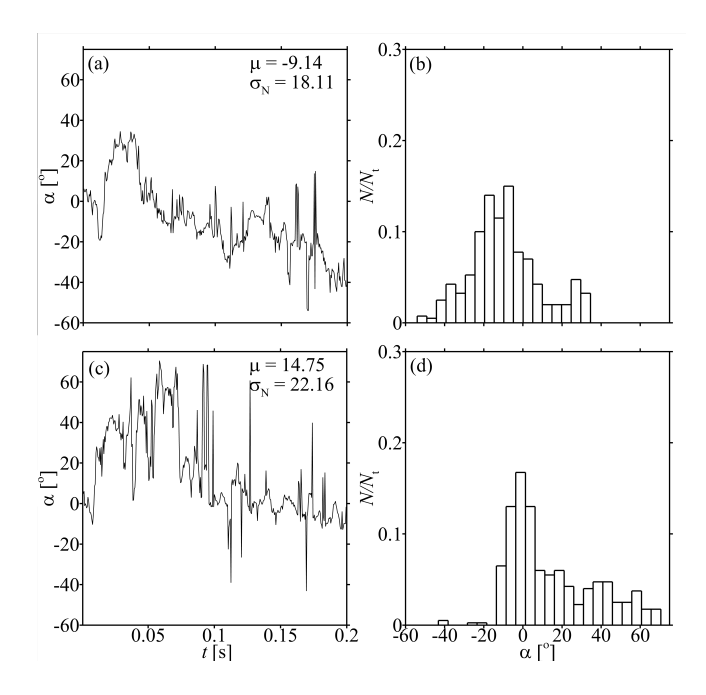


FIGURE 5. THE JET ANGLE VARIATION AND THE HISTOGRAM DISTRIBUTIONS FOR 0.2 s SUSTAINED PRONUNCIATION OF [F] AT SUBGLOTTAL PRESSURES OF (a)-(b) 300 AND (c)-(d) 860 Pa.

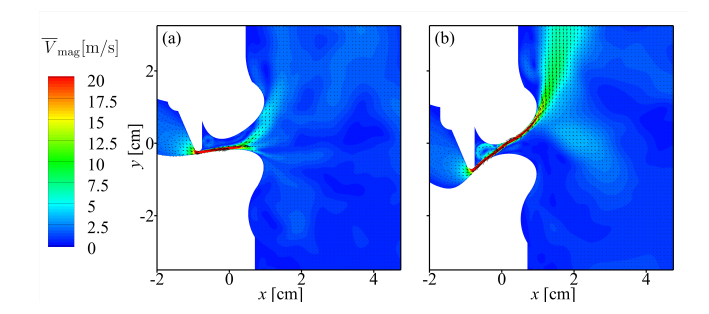


FIGURE 6. THE MEAN VELOCITY CONTOURS IN CONJUCTION WITH THE MEAN VELOCITY VECTORS AT 0.2 s FOR THE (a) FLAT-[F] AND (b) CURVED-[F] MODEL AT A SUBGLOTTAL PRESSURE OF 600 Pa.

confirms that the jet stays attached to the upper lip producing predominantly positive-oriented jet trajectories.

DROPLET PROPAGATION

To highlight the effects of speech flow trajectories direction on the pattern of droplet propagation, droplets with diameters of 0.1 to 50 μm were introduced from the tooth gap region with an injection rate of $1\times 10^5~s^{-1}$ and an initial velocity equal to that of the local fluid. The distributions of droplets were quantified

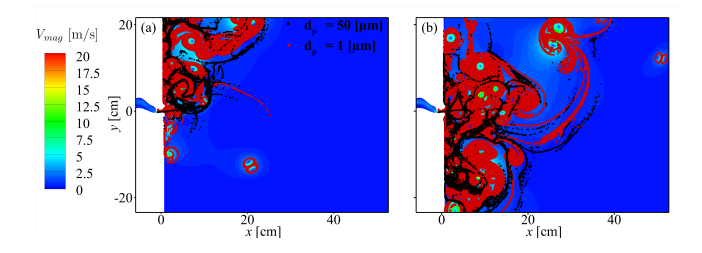


FIGURE 7. THE DISTRIBUTION OF 0.1 AND 50 μm DROPLETS AFTER (a) 0.2 s AND (b) 0.4 s PERIOD OF DROPLET PROPAGATION FROM THE FLAT-[F] MODEL AT A SUBGLOTTAL PRESSURE OF 600 Pa.

during the 0.4 s period of the expiration. To clarify the evolution of droplet propagation during sustained fricative [f] articulation, the distributions of droplets at 0.2 and 0.4 s of [f] production from the flat-[f] model at a subglottal pressure of 600 Pa are shown in Figure 7.a and 7.b, respectively. As it was discussed earlier, the predominant direction of airflow propagation duration the initial period of 0.15 s is mainly upward so that as it is seen in Figure 7.a droplets are spread in the upper region of the speaker at 0.2 s. However, as a result of negative airflow trajectories during the period of 0.2 to 0.4 s, droplets are transported and propagated into the lower region of the surrounding domain. To highlight the different behavior of large and small size droplets, distributions of 0.1 and 50 µm droplets, where the red and black dots represent 0.1 and 50 µm droplets, respectively, were shown simultaneously in the figures. The different behavior of larger and smaller droplets is clear in the figures. The figures clarify smaller droplets can follow the small-scale flow structures and spread in different directions, but large droplets initially have a ballistic-like motion and then spread by large-scale structures of the airflow field. The figures also illustrate the rule of vortex structures in spreading smaller droplets (0.1 µm) to the far-field. The influence of gravitational effects on large size droplets (e.g., 10-50 µm) was not observed since they were under influence of large velocity expiratory flow, but if the expiratory flow stops or they move to the far-field regions, large droplets will settle to the ground.

ACKNOWLEDGEMENTS

This work was supported by the National Science Foundation under grant number CBET:2029548.

CONCLUSIONS

By simulation of airflow through vocal tract geometries generated based on real-time MRI data during production of [f] utterance, the complex unstable behavior of expirated flow for fricative [f] utterance was highlighted. It was found that the flow is

significantly affected by the subglottal pressure (i.e., loudness) and the lips shape. This investigation revealed that during fricative [f] production, a very unstable jet flow with a large velocity appears at the constriction region located between the lower lip and the upper teeth whose predominant direction is remarkably affected by the loudness and the curvature of the tip tongue and the lower lip. It was found that for loud utterance, the airflow trajectories and the spread direction of speech droplets tend to be more upward in comparison to those produced by soft utterance. Due to the upward slope of the curved model, the airflow trajectories maintain their positive angles, hence droplets are also spread more towards the upper regions of the flow region which increases the chance of speech droplets traveling farther distances before falling to the ground.

REFERENCES

- [1] for Disease Control, C., Prevention, et al., 2020. Scientific brief: Sars-cov-2 and potential airborne transmission.
- [2] Morawska, L., and Milton, D. K., 2020. "It is time to address airborne transmission of coronavirus disease 2019 (covid-19)". *Clinical Infectious Diseases*, 71(9), pp. 2311–2313.
- [3] Abkarian, M., Mendez, S., Xue, N., Yang, F., and Stone, H. A., 2020. "Speech can produce jet-like transport relevant to asymptomatic spreading of virus". *Proceedings of the National Academy of Sciences*, 117(41), pp. 25237–25245.
- [4] Chao, C. Y. H., Wan, M. P., Morawska, L., Johnson, G. R., Ristovski, Z., Hargreaves, M., Mengersen, K., Corbett, S., Li, Y., Xie, X., et al., 2009. "Characterization of expiration air jets and droplet size distributions immediately at the mouth opening". *Journal of Aerosol Science*, 40(2), pp. 122–133.
- [5] Asadi, S., Wexler, A. S., Cappa, C. D., Barreda, S., Bouvier, N. M., and Ristenpart, W. D., 2019. "Aerosol emission and superemission during human speech increase with voice loudness". *Scientific reports*, *9*(1), pp. 1–10.
- [6] Yoshinaga, T., Nozaki, K., and Wada, S., 2019. "Aeroacoustic analysis on individual characteristics in sibilant fricative production". *The Journal of the Acoustical Society of America*, **146**(2), pp. 1239–1251.
- [7] Narayanan, S., Toutios, A., Ramanarayanan, V., Lammert, A., Kim, J., Lee, S., Nayak, K., Kim, Y.-C., Zhu, Y., Goldstein, L., et al., 2014. "Real-time magnetic resonance imaging and electromagnetic articulography database for speech production research (tc)". *The Journal of the Acoustical Society of America*, 136(3), pp. 1307–1311.
- [8] Narayanan, S. S., Alwan, A. A., and Haker, K., 1995. "An articulatory study of fricative consonants using magnetic resonance imaging". *The Journal of the Acoustical Society of America*, **98**(3), pp. 1325–1347.
- [9] Hamlet, S. L., Cullison, B. L., and Stone, M. L., 1979.

- "Physiological control of sibilant duration: Insights afforded by speech compensation to dental prostheses". *The Journal of the Acoustical Society of America*, **65**(5), pp. 1276–1285.
- [10] Mofakham, A. A., Helenbrook, B. T., Erath, B. D., Ferro, A. R., Ahmed, T., Brown, D. M., and Ahmadi, G., 2021. "On variability of expiratory airflow dynamics due to vocal tract geometrical variations and speech loudness". Submitted in Aerosol Science and Technology.